EIFS Hygrothermal Performance Due to Initial Construction Moisture as a Function of Air Leakage, Interior Cavity Insulation, and Climate Conditions

Mikael H. Salonvaara
Member ASHRAE

Achilles N. Karagiozis, Ph.D.
Member ASHRAE

ABSTRACT

The drying capability of an EIFS wall system with initial construction moisture critically depends on the climatic conditions in which it is placed. The drying rate mechanisms with which walls redistribute and transport moisture away from the envelope may affect the service life of the wall system. Potential moisture-induced damage becomes important when the wall is not properly designed with adequate drying capacity.

This paper investigates the drying performance of a particular EIFS (exterior insulation and finish system) clad wall. A state-of-the-art two-dimensional hygrothermal model, developed by the authors, was employed to determine the hourly spatial temperatures, moisture content, and air velocity distributions within wall systems as a function of real climatic conditions.

In the parametric investigation, the performance of a particular EIFS clad wall as a function of two stud cavity insulation materials was studied. Two cavity insulation materials were investigated: fiberglass and cellulose insulation. Two climatic conditions were chosen in the moisture analysis, representing cold and mild climates; these were Chicago, Illinois, and Wilmington, North Carolina, respectively.

The effect of wall drying and wetting in the presence of a particular airflow path (cracks) was investigated for all cases. The air leakage path was assumed to be present due to an electrical outlet close at the interior, an opening present between oriented strand panels, and a conduit in the stucco layer. Initial OSB moisture content was assumed to be very high. The influences of wind-driven rain, solar radiation, and air movement were included in the simulation analysis on an hourly basis.

Results showed that air leakage through a particular EIFS clad wall in Wilmington produced a net drying effect for a wall system with an initially wet OSB layer, while air leakage developed a net seasonal moisture accumulation in Chicago. The effect of stud cavity insulation was found to be critical, as the storage capacity for moisture increased in the cellulose case, compared to the fiberglass insulation case. The distinct effect is present when comparing the two insulation systems. The cellulose insulation case retained higher amounts of moisture. Solar-driven moisture was also more critical in the cellulose insulation case than in the fiberglass case. The thermal and moisture results were then linked to a state-of-the-art mold growth model to assess the risk of moisture-induced damage. Results were developed in the form of mold growth indexes. Results showed the probable mold growth index potential as a function of climatic conditions and as a function of cavity insulation. Higher risk of mold growth is present in the cellulose case than in the fiberglass insulation case. If there is a high mold growth index and the underlying material is maintained at high moisture content, there is a potential for developing decay (if the wood is already infected internally). Since boric acid is added in cellulose insulation as a treatment for fire, mold, and insect and rodent control, as wet blown cellulose comes in contact with other materials, some of the chemical will treat these surfaces. For the same wall system, Wilmington exhibited slightly worse conditions than Chicago for mold growth. The development of mold growth indexes permits one to perform a moisture engineering analysis and extend current moisture assessment analysis of building envelopes' long-term performance.

INTRODUCTION

Many severe durability problems can be traced to the presence of moisture. In many cases, one can distinguish a critical moisture content above which durability problems may occur and below which problems are small. Depending on the wall system and environmental conditions in which the wall is placed, different time-dependent degradation mechanisms may be present if the quantity of moisture exceeds certain material system and material subsystem thresholds.

Mikael H. Salonvaara is a research scientist with VTT Building Technology, Espoo, Finland. **Achilles N. Karagiozis**, previously with the National Research Council Canada, is currently a senior research engineer with the Oak Ridge National Laboratory, Oak Ridge, Tenn.

Moisture can be present in any wall system in three thermodynamic physical states: the solid state (ice), the liquid state, and the vapor state. Indeed, all three may be present concurrently in a wall system. This makes the fundamental transport interactions within a construction material complex. Understanding the overall performance of building envelope systems with respect to heat, air, and moisture, excluding durability, is a formidable task. Currently, due to limited experimental capabilities to measure moisture transport potentials in situ, one needs to resort to advance modeling with heavy reliance on accurate material and material subsystem properties to quantify wall heat, air, and moisture performances.

A wall system can be characterized with a few basic systems. The most exterior subsystem is identified as the cladding, or façade, system. Others are the drainage (capillary break) or ventilation system, the sheathing system, the insulation system, the framing system, the vapor diffusion control system, and the air barrier system. A multitude of variations exist along these fundamental systems, but in some cases several of the systems can be represented by one system if proper performance criteria can be satisfied.

In this paper, emphasis is placed on the effect of the performance of an air barrier system and the influence of cavity insulation material properties on the drying performance of an EIFS clad wall in two climatic conditions. Many authors have indicated that airtightness through a wall assembly is the most important performance criterion that a building envelope must satisfy (TenWolde and Rose 1996). Airtightness is defined here as the amount of air that leaks through a building envelope at specified pressure differences. Lack of airtightness in wall systems can lead to increased risk of moisture damage and a major degradation of energy efficiency (Ojanen and Kumaran 1996). Lightweight construction such as wood frame wall systems seldom achieves perfect airtightness (Janssens and Hens 1996). In theory, an adequate air barrier system could prevent leakage, and this would prevent moisture-induced damage. However, in practice, a perfect air barrier is impossible to achieve because small defects such as perforations or cracks can destroy its intended efficiency.

In a recent study (Hamlin and Gusdorf 1997), it is reported that major progress has been achieved in Canada with respect to achieving higher airtightness levels since 1921. The Canadian national average airtightness for a conventional home built in 1921 was 12.19 air changes per hour (ACH); in 1961, 6.11 ACH; and in 1991, 3.10 ACH at 50 Pa pressure differences. An advanced house such as the R-2000 homes is documented with an average national airtightness of 1.24 ACH at 50 Pa pressure difference.

Regarding residential buildings, the literature refers to airtightness of the building envelope with a specific value that is considered to be constant throughout the year. However, the field evaluation work by Warren and Webb (1986), Persily (1986), and Kim and Shaw (1986) clearly indicates that a seasonal variation of airtightness, ranging between 20% and 40% depending on climatic conditions, is present. Kim and Shaw (1986) developed a correlation of seasonal variation of airtightness as a function of relative humidity.

Air leakage can be a dominant factor in the transport of heat and moisture through building envelope systems. Deterioration of envelope systems can in many instances be attributed solely to the moisture transported by air leakage (Ojanen and Kumaran 1992). In cold climates, the interior normally has higher water vapor pressures during the winter than the exterior. Depending on the effect of stack pressures, interior mechanical pressures, and wind pressures, positive or negative pressure differentials can exist between the inside and the outside of the envelope. The presence of pressure differentials drives quantities of air through intentional and unintentional openings (cracks). Depending on the temperature distribution and the air passage routes through and around the various material sections in the wall envelope, moist air can condense. This accumulation of moisture due to convective flow can be many times more important than the vapor accumulation due to diffusion transport. Experimental work detailing the airflow paths within walls has not yet been developed, and information is generally lacking. The amount of available information regarding the hygrothermal performance of wall systems due to air leakage flow is very minimal, with the exception of the numerical work by Ojanen and Kumaran (1992, 1996) for cold climates. To date, limited information is available for EIFS walls located in mixed climatic conditions.

Serious moisture problems in EIFS clad walls in the New Hanover County area of North Carolina have appeared (Nisson 1995). Moisture problems ranging from high moisture content in the exterior sheathing to severe decay were uncovered. Most of the catastrophic failures have been traced to the existence of liquid water and the inability of the wall system to dry out within a critical time. As wood products are employed in wood frame construction, wood rotting and mold growth can occur if favorable conditions are present (Viitanen 1996).

In a recent paper by Karagiozis and Salonvaara (1998), the performance of a particular EIFS clad wall system was investigated as a function of three interior vapor control strategies and two air leakage rates. Results were developed for a mixed climate, such as that found in Wilmington. Results drawn from that study assessed the effect of air leakage for one wall orientation through the assumed airflow path. Air leakage through an EIFS clad wall in Wilmington produced a net drying effect for a wall system with an initially wet OSB layer. Vapor diffusion control strategies were also found to have a significant effect on the hygrothermal performance (drying potential) of EIFS clad walls for mixed climatic conditions. The study recommended additional research to address the drying performance of wall systems in various climatic conditions and the influence of different cavity insulations.

OBJECTIVES OF PRESENT STUDY

This work is concerned with the hygrothermal performance (drying potential) of a particular EIFS clad wa

subjected to a specific air leakage flow path. The heat, air, and moisture performance of the wall systems were investigated as a function of two cavity insulations: fiberglass insulation and cellulose insulation. The objective of the work was to determine the hygrothermal performance of the wall structure for two different climatic conditions and cavity insulation materials. A cold and a mixed climate were selected for the study, and these were: Chicago, Illinois, and Wilmington, North Carolina. The analysis was conducted while subjecting the exterior boundary to real weather data (including temperature, vapor pressure, wind speed and orientation, solar radiation, wind-driven rain, sky radiation, and cloud indexes) by employing a moisture analysis approach that blends intensive numerical analysis and measured material properties.

MATERIAL PROPERTY DETERMINATION

Hygrothermal material properties for some of the materials of the EIFS clad wall were measured, and detailed material property results are available in papers (Karagiozis and Kumaran 1997) and within the material database of LATENITE (Karagiozis et al. 1994). The basic material properties required in the modeling analysis are

- water vapor permeance,
- liquid diffusivity,
- sorption plus suction isotherm, and
- thermal conductivity, density, and heat capacity.

These properties are not singly valued but may be dependent on temperature and/or moisture content. Directionally dependent material properties were employed for the wood-based and insulation materials.

DESCRIPTION OF THE HYGROTHERMAL MODEL

The LATENITE 1.3 model includes the porous airflow through insulation and cracks by solving a subset of the Navier-Stokes equations and Darcy's equations, a detailed description of which is given by Karagiozis (1997). Vapor and liquid transport are solved simultaneously. A detailed description of the 1.0 model is given by Hens and Janssens (1993) and Karagiozis (1993); version 1.2 is described by Salonvaara and Karagiozis (1994). The moisture transport potentials used in the model are moisture content and vapor pressure; for energy transport, temperature is used. The model was developed by the authors and has been tested and validated for numerous hygrothermal transport applications.

DESCRIPTION OF MOLD GROWTH MODEL

Mold growth in the structures was estimated using a model equation that employs temperature, relative humidity, and exposure time as input. The mold growth model and differential mathematical equations were developed and presented in detail by Hukka and Viitanen (1998) and Viitanen (1997a, 1997b), and only a short description is given here.

Quantification of mold growth in the model is based on the mold index first employed in biological experiments during visual inspection (Viitanen 1996). The mold growth model is based on mathematical relations for the growth rate of mold in different conditions, including the effects of exposure time, temperature, relative humidity, and dry periods. The model is purely mathematical in nature, and, as mold growth was only investigated with visual inspection, it does not have any connection to biology in the form of modeling the number of live cells. Also, the mold index resulting from computations with the model does not reflect the visual appearance of the surface under study because traces of mold growth remain on a wood surface for a long time. The correct way to interpret the results is that the mold index represents possible activity of the mold fungi on a wood surface.

The model makes it possible to calculate the development of mold growth on the surface of wooden samples exposed to fluctuating temperature and humidity conditions including dry periods. The numerical values of the parameters included in the model are fitted for pine and spruce sapwood, but the functional form of the model can be considered valid for other wood-based materials also.

The mold index scale employed in the analysis is explained in Table 1.

TABLE 1
Mold Index Values and Description

Index	Descriptive Meaning
0	No growth
1	Some growth detected only with microscope
2	Moderate growth detected with microscope
3	Some growth detected visually
4	Visually detected coverage more than 10%
5	Visually detected coverage more than 50%
6	Visually detected coverage 100%

PROBLEM DESCRIPTION

The hygrothermal performance of a particular EIFS clad wall, depicted in Figure 1, was analyzed. This wall is the same as the one investigated by Karagiozis and Salonvaara (1998). Only one air leakage characteristic (air leakage opening size) was investigated. An air opening of 3 mm throughout the depth was used and labelled as Case 1. This case represents a possible air gap present when the drywall is employed as the air barrier system (Straube 1998). An airflow rate of 0.5 L/(m^2·s) is present when a static pressure difference of 75 Pa is applied to the EIFS wall. Even small gaps such as the ones employed in this study permit coupling of the interior and exterior environments. This alone demonstrates the sensitivity of the presence of air gaps in the wall system on the air leakage behavior of walls.

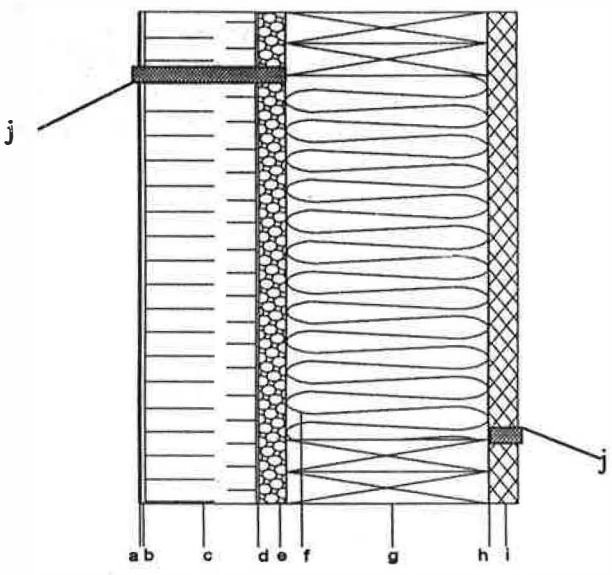

Figure 1 *The analyzed wall structure in detail: (a+b) 5 mm base and finish coating, (c) 50 mm expanded polystyrene board, (d) 1 mm glue layer, (e) 12.5 mm oriented strand board, (f) 89 mm fiberglass insulation, (g) 76 mm thick double bottom and top plate, (h) the vapor control layer, (i) 12.5 mm gypsum board, (j) 1 mm or 3 mm air opening.*

The air opening provided the main path for air leakage flow through the wall system. No direct water entry through these openings was permitted; however, wind-driven rain was permitted through the exterior face of the wall. One interior vapor control strategy was employed, using a 6 mil polyethylene as a vapor barrier.

A solid EIFS clad wall (no-window details) was selected for the numerical analysis. The wall is centrally located in the middle of a two-story building and is composed of the following layers starting from the exterior to interior: 5 mm lamina, 50 mm expanded polystyrene board, 1 mm adhesive coating, 12.5 mm oriented strand board, 89 mm fiberglass insulation, 76 mm thick double bottom and top plate, the vapor control layer (6 mil polyethylene), and 12.5 mm painted gypsum board. The air leakage gaps (1 mm or 3 mm) are also shown. The inside surface of the gypsum board was coated with a vapor permeable paint (permeance approximately 200 ng/(m^2·s·Pa) or 4 perms). The oriented strand board moisture content was initially assumed to be 44%. This represents a very wet initial moisture condition in the OSB layer, which would be above acceptable moisture content permitted by building inspectors. However, this moisture content can be present when the OSB is wetted directly by rain. All other layers in the wall system were assumed to be in equilibrium at 80% relative humidity.

Wind-driven rainwater was included in the analysis; the exterior surface was exposed to the amount of rain that hits a vertical wall. This amount depends on the intensity of precipitation, wind speed and direction, as well as the location on the wall surface. Wind-driven rain was used in the analysis as calculated by employing a commercially developed model (ASC 1993).

The wall was exposed to outside air temperature and the relative humidity that varied according to the weather data from the selected locations of Wilmington and Chicago. The simulations were carried out for a one-year exposure (365 days) starting on the 1st of October. The solar radiation and longwave radiation from the outer surfaces of the wall were included in the analysis.

BOUNDARY CONDITIONS

Internal conditions were kept constant at a temperature of 21°C and relative humidity of 45% RH (Pv = 1119 Pa) throughout the year. U.S. National Climatic Center (NCC 1995) data for the years 1961-1962 were used in the simulations. The monthly average temperatures and vapor pressures and vapor pressure differences ($P_{exterior} - P_{interior}$) for Wilmington and Chicago are shown in Figures 2a and 2b. The yearly average temperature and vapor pressure in Wilmington is 18.5°C and 1788 Pa and in Chicago, 10.2°C and 1108 Pa for the simulated period.

The 30-year average (1961-90) temperature and exterior vapor pressure for Wilmington is 17.16°C and 1623 Pa and for Chicago, 9.64°C and 1008 Pa. The modeled wall located on the second floor of the building was facing south. The glue layer was simulated as a water-retaining material with capillaries of greater than 1.0 mm. This layer permitted the storage of liquid water and a high gravity moisture transport. The heat and mass transfer coefficients for external and internal surfaces were assigned values that varied from hour to hour depending on the exterior weather wind speed and orientation conditions and interior conditions.

Air leakage through the wall system was determined on an hourly basis, based on the combined effect of stack and wind pressure. Solar radiation, cloud coverage, and sky radiation effects were also included in the model. All simulations were conducted using a two-dimensional wall cross section with adiabatic conditions for both thermal and moisture transport at the bottom and top horizontal surfaces.

SIMULATION RESULTS

In this section, the results will be discussed for the particular EIFS clad wall with the prescribed air leakage path for the two climatic conditions and cavity insulations.

Air Leakage Characterization

In Figures 3a and 3b, the number of hours in which the wall is subjected to an infiltration or exfiltration flow is plotted for Chicago and Wilmington environmental conditions. In both cases, fiberglass insulation was employed. It is obvious that the two climatic locations exhibit different directions of air leakage during the year, Chicago having a higher percent-

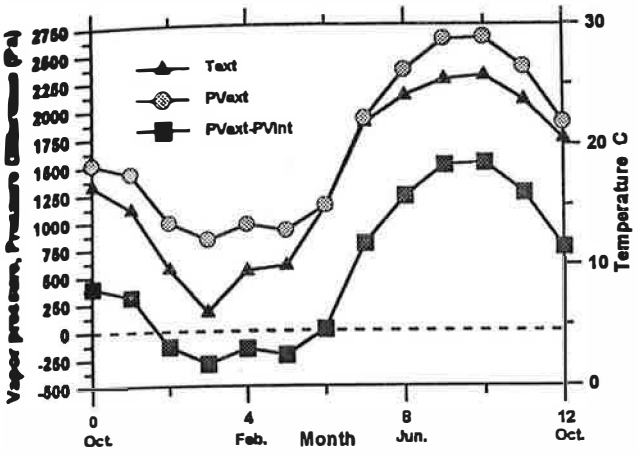

Figure 2a The monthly average temperatures, vapor pressures, and vapor pressure difference (exterior-interior) for Wilmington weather conditions for a period of 18 months (1961-1962).

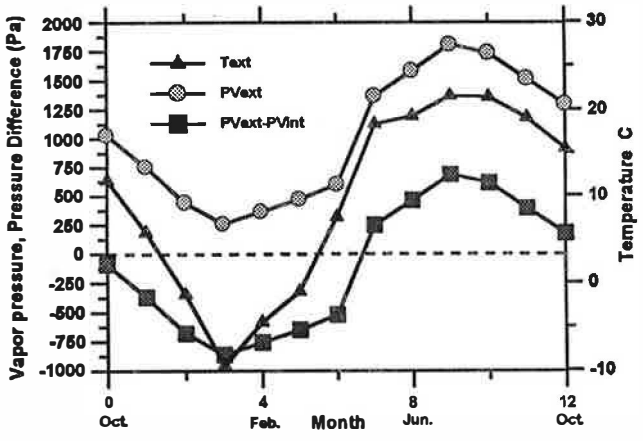

Figure 2b The monthly average temperatures, vapor pressures, and vapor pressure difference (exterior-interior) for Chicago weather conditions for a period of 18 months (1961-1962).

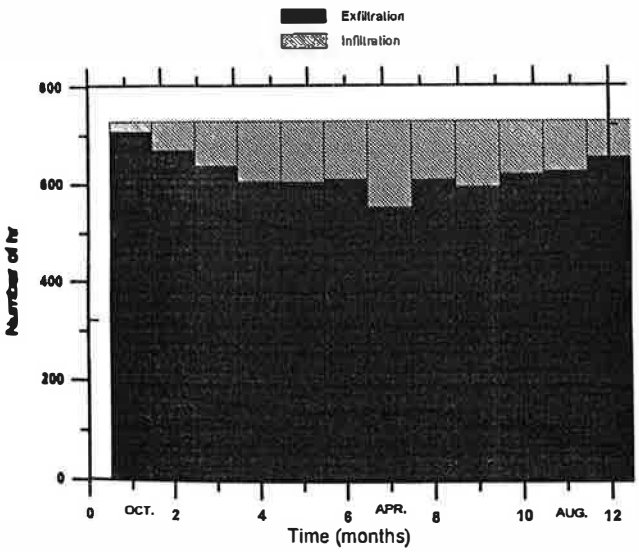

Figure 3a Distribution per month for infiltration/ exfiltration air leakage (Wilmington).

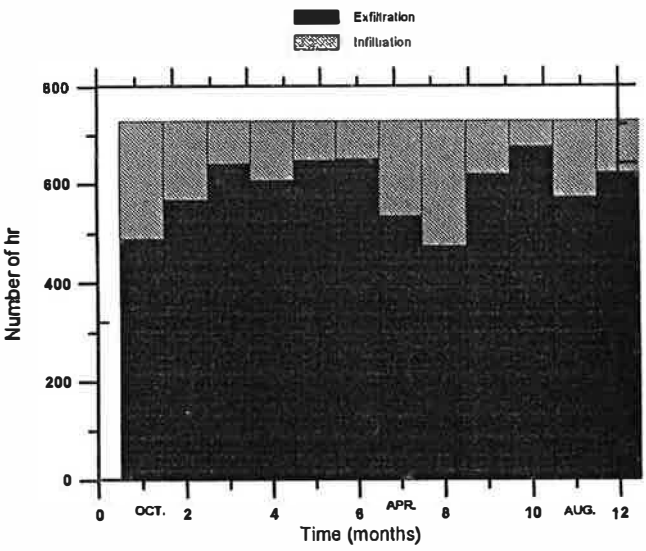

Figure 3b Distribution per month for infiltration/ exfiltration air leakage (Chicago).

age of the time with air leakage toward the interior than Wilmington. From these two figures, to characterize the heat, air, and moisture performance of a particular wall system, one must include the effects of wind in the analysis as these may be different as shown between the locations of Chicago and Wilmington. Figures 4a and 4b display the monthly maximum, minimum, and average mass flow through the wall system for the cities of Wilmington and Chicago, respectively. Figures 5a and 5b show the instantaneous hourly mass flows through the wall system for climatic conditions in Wilmington, for the two different cavity insulations employed. As the air permeability of the cellulose insulation is ten times less than that of the fiberglass insulation, the air leakage through the envelope decreases considerably. The air permeability of blown-in cellulose depends on the density of the insulation and whether it is wet or dry blown. Cellulose products do exist that have lower air permeability.

Moisture Characterization

In Figure 6, the total amount of moisture present in the wall system as a function of time is presented to show the relative hygrothermal performance of the EIFS wall for the two different climatic conditions and cavity insulations. The wall system that employed cellulose cavity insulation showed the slowest drying. The wall that was simulated with Chicago

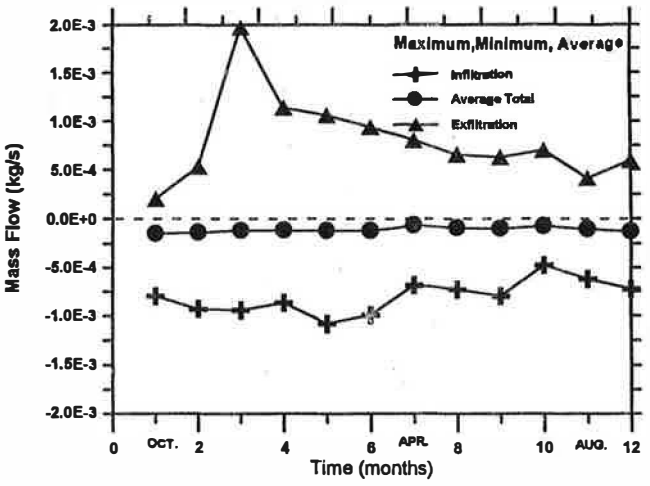

Figure 4a *Average total mass flows, average infiltration flow, and average exfiltration flow (Wilmington).*

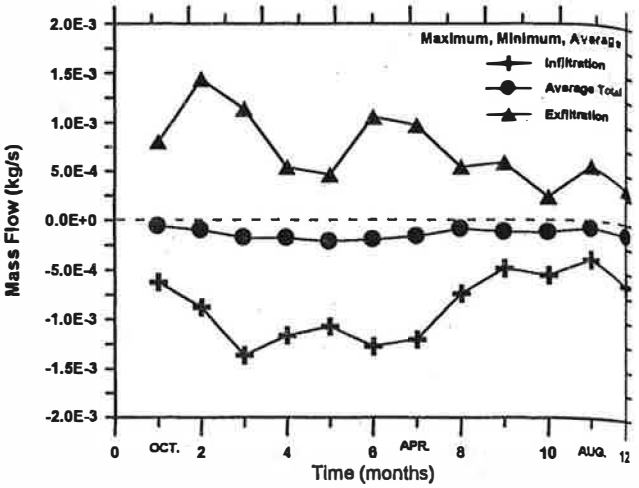

Figure 4b *Average total mass flows, average infiltration flow, and average exfiltration flow (Chicago).*

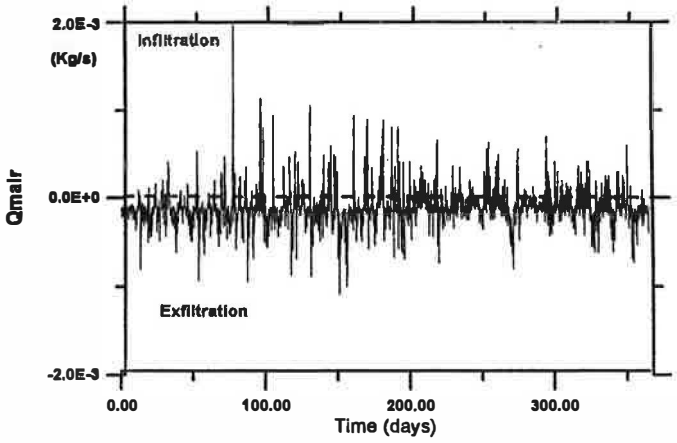

Figure 5a *Air leakage through wall section with a 1 mm air gap (fiberglass).*

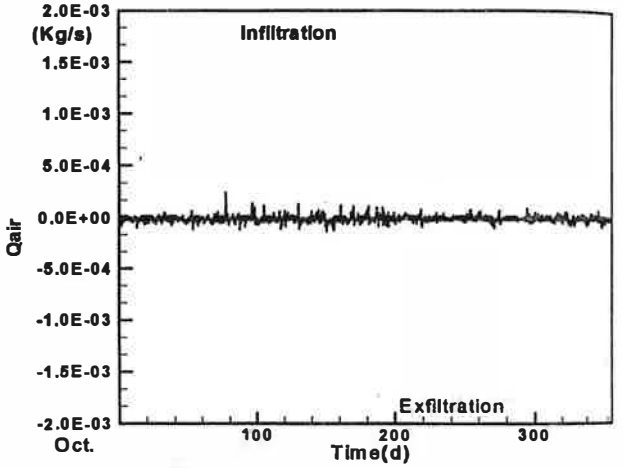

Figure 5b *Air leakage through wall section with a 1 mm air gap (cellulose insulation).*

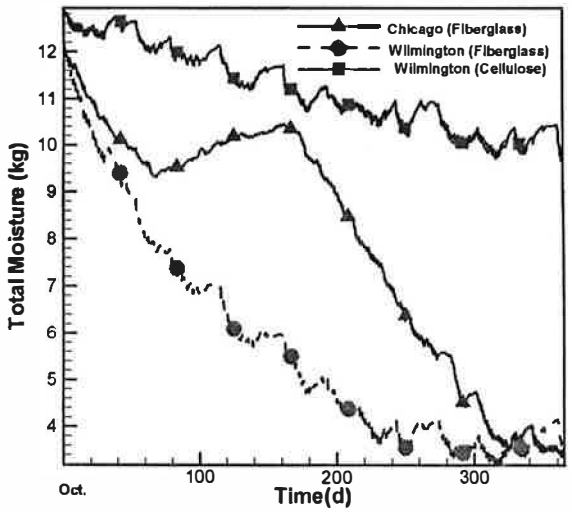

Figure 6 *Total moisture in the wall as a function of insulation and weather location.*

conditions displayed slower drying than the one located in Wilmington. The wall system in Chicago, insulated with fiberglass, exhibited a temporary net accumulation, starting in mid-December, for approximately 3.5 months during the winter period. The influence of air leakage on the hygrothermal performance of a leaky wall system in a cold climate is evident. A seasonal moisture accumulation was present even when the wall already had high quantities of moisture present. This confirms the importance of maintaining proper air leakage control in cold climates.

Figure 7 shows the transient total moisture in the oriented strand board sheathing in Wilmington for three cases—the cases that employed fiberglass and cellulose insulation with air leakage and the case with fiberglass insulation without air leakage. The most rapid drying is observed for the fiberglass insulation case with air leakage, followed by the fiberglass case without air leakage present, and cellulose. The sorption characteristics of cellulose insulation, which permits higher

accumulation of moisture, develop slower drying of the OSB layer. Similarly, Figure 8 compares the transient moisture content of the OSB layer as a function of time for Wilmington and Chicago for fiberglass insulation, as well as cellulose in Wilmington. Time equal to zero coincides with October 1, 1961. The drying potential for these two climatic conditions is also clearly depicted—the wall located in Chicago stored substantially higher amounts of moisture over the year than the one in Wilmington. At the end of the year (October 1963), differences between these two climatic conditions are insignificant. However, the wall that employed cellulose insulation did not permit the OSB layer to dry out to the same level as fiberglass insulation.

In Figure 9, the transient relative humidity distribution is shown as a function of time for the top and bottom wood cavity plates in Wilmington, when fiberglass insulation is employed. Initially, the wood plates were in equilibrium at 80% relative humidity. Results are shown after the first week, for four locations, each 1 mm away from the ends of the wood plate (polyethylene and OSB) and 1.5 mm away from contact with the insulation. Locations 1 and 3 are the closest to the exterior of the wall. The results clearly depict a multidimensional moisture distribution within the wood plates. The two locations close to the inside of the wall show considerably lower relative humidities present. The bottom outer location exhibits higher moisture contents than the top outer location.

Figure 10 shows the transient relative humidity distribution at the innermost location of the OSB layer as a function of three heights. The three vertical locations correspond to 0.1 m, 1.0 m, and 2.0 m from the bottom of the OSB. Initially, a difference (≈10%) between the bottom and top locations was present; this difference became negligible after a one-year

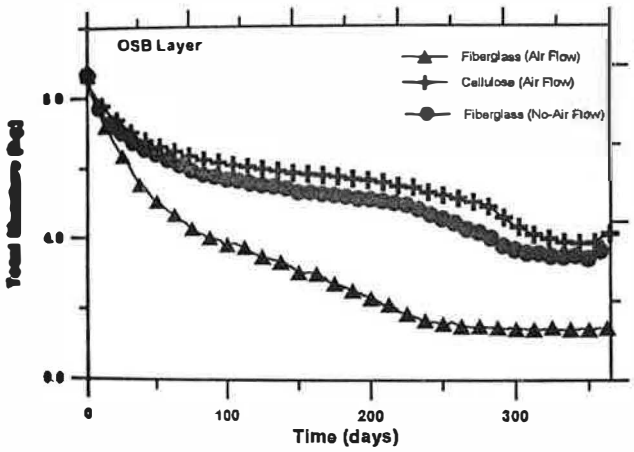

Figure 7 *Characteristic OSB drying rate curves for 1 mm air opening case.*

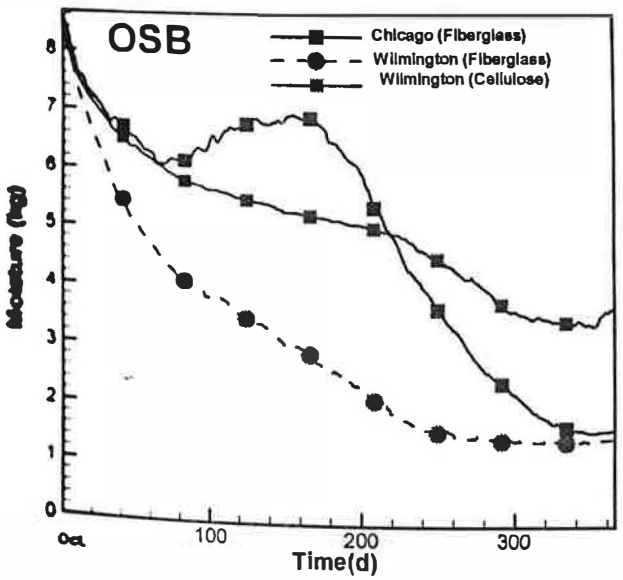

Figure 8 *Characteristic OSB drying rate curves for 1 mm air opening case.*

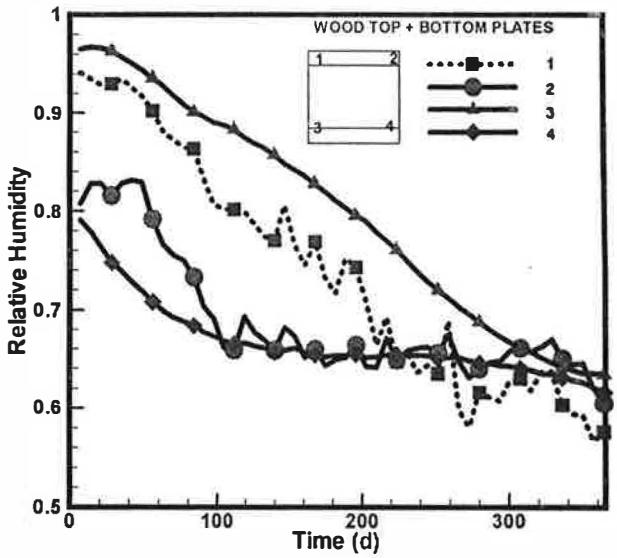

Figure 9 *RH transient distribution in top and bottom plates (fiberglass insulation, Wilmington).*

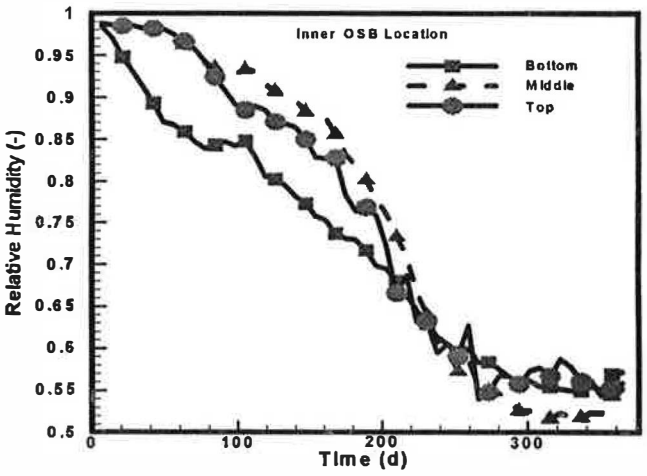

Figure 10 *RH transient distribution in top and bottom plates (fiberglass insulation, Wilmington).*

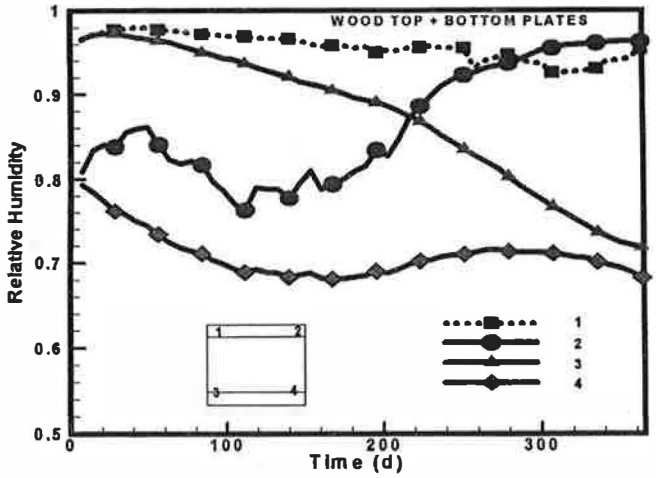

Figure 11 RH transient distribution in top and bottom plates (cellulose insulation, Wilmington).

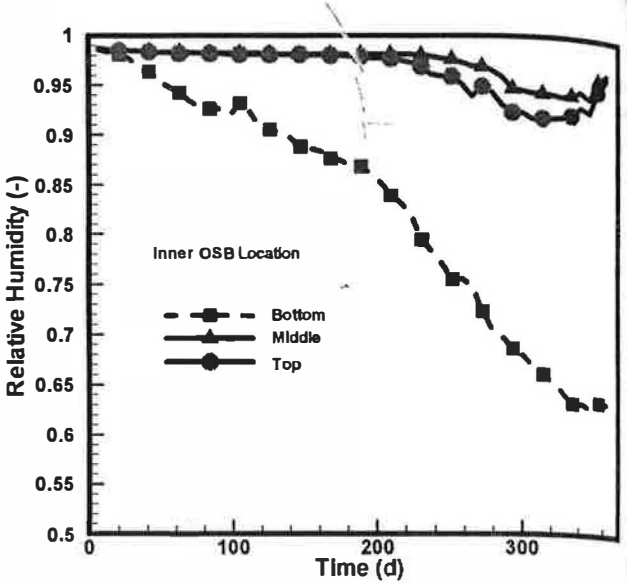

Figure 12 RH transient distribution in top and bottom plates (cellulose insulation, Wilmington).

period. However, the middle location displayed higher relative humidities starting in the winter period and extending this interval until July. The forced air leakage through the wall, coupled with natural convection, is mainly attributed to this vertical distribution.

Similarly, in Figure 11, the transient relative humidity distribution is shown as a function of time for the top and bottom wood cavity plates in Wilmington when cellulose insulation is employed. The results clearly depict a multidimensional moisture distribution within the wood plates that is more prominent than in the fiberglass insulation case. The air leakage through the wall assembly is considerably reduced by the presence of cellulose insulation. The two top locations in the wood plate show considerably higher relative humidities present. The inner top location shows a net accumulation trend over the full one-year simulation period that is most likely due to solar-driven moisture.

Figure 12 shows the transient relative humidity distribution at the innermost location of the OSB layer as a function of the same three height locations. A distinct vertical relative humidity distribution is apparent with the highest relative humidity present at the top location, followed by the middle, and with the lowest at the bottom.

Mold Growth Analysis

To assess the mold growth potential, the hourly thermal and moisture distributions in the wall assembly were included in a mold growth model. The Hukka and Viitanen (1998) mold growth index model was incorporated into the LATENITE model. The interpretation of the mold growth index was presented earlier in Table 1. Figures 13, 14, and 15 show the mold growth indexes for the top and bottom plates of the same four locations for which relative humidity data were presented previously: for the Wilmington fiberglass, Wilmington cellulose, and Chicago fiberglass insulation cases, respectively.

In Figure 13, the mold growth index for the innermost locations at both the top and bottom locations shows negligible mold growth during the full year. At the top outermost location, the mold index rises to a maximum value after 40 days from October and does not exceed level 4 (this corresponds to a visually detectable mold growth area of not more than 10%). The bottom outermost location displays higher mold growth index potential, ranging within level 5. Both outermost locations have reduced risk of mold damage at the end of the year, dropping to levels 3 and 1 for the top and bottom outermost locations, respectively. Figure 14 displays the mold growth index results for the cellulose insulation case. It is evident that the mold growth indexes for the three locations—top outermost, top innermost, and bottom outermost—

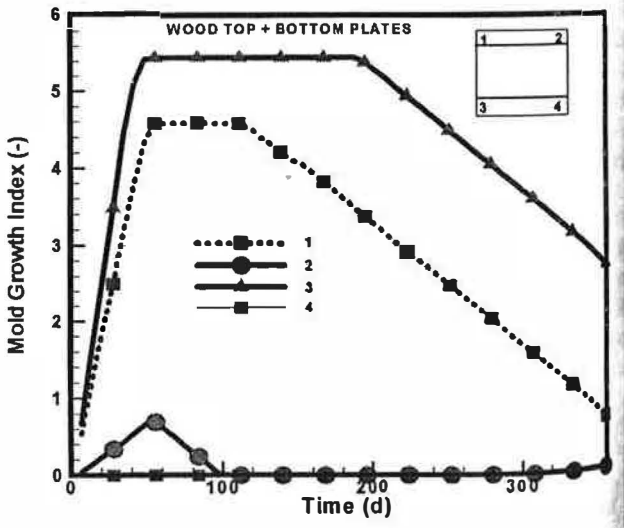

Figure 13 Mold growth index for fiberglass case (Wilmington).

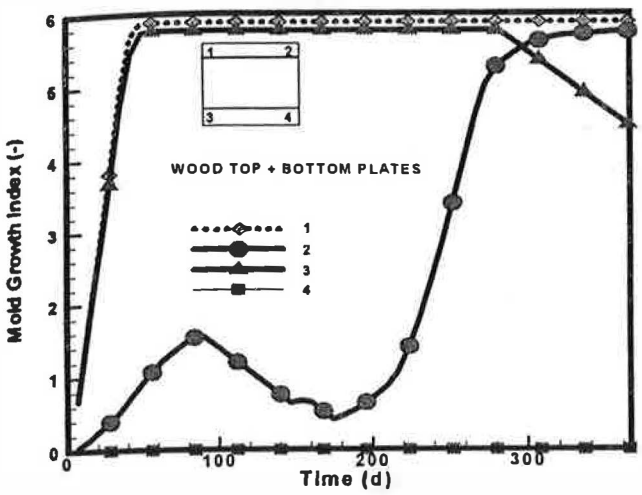

Figure 14 Mold growth index for the cellulose case (Wilmington).

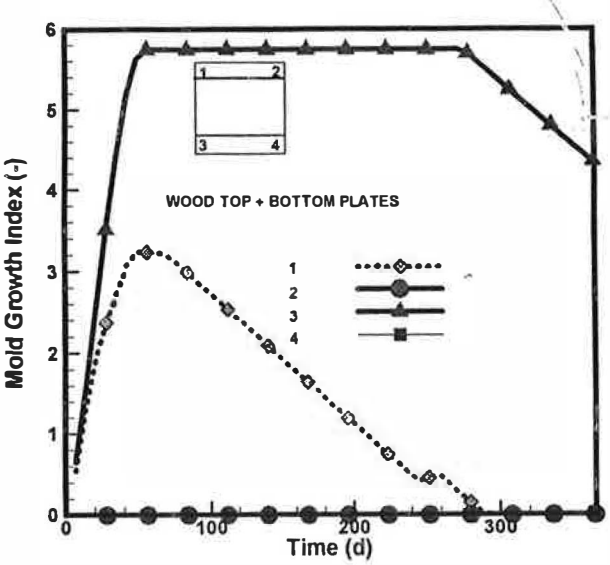

Figure 15 Mold growth index for the fiberglass case (Chicago).

display critical levels of mold growth indexes. Indeed, results from the top outermost location throughout the one-year period display mold growth indexes close to 6 (very high potential activity of mold growth). In addition, the bottom outermost location shows an increasing trend for mold growth index as a function of time. Finally, Figure 15 shows the mold growth index for the Chicago case employing fiberglass cavity insulation. Results show no potential for growth of mold for the bottom and top innermost locations and highest mold growth in the bottom outermost location followed by the top outermost location. From the mold growth index analysis for the three cases shown in Figures 13 - 15, the potential for moisture-induced problems due to initial construction moisture is critical.

CONCLUSIONS

The intent of this study was to determine the hygrothermal performance of a particular EIFS clad wall, starting with initially high construction moisture in the OSB layer and with an assumed airflow path. Diffusion drying rates of any wall system are essentially controlled by the water vapor permeance properties of all critical layers of the wall system, exterior lamina, expanded polystyrene, OSB layer, insulation layer, vapor barrier, and interior paint coating. This study investigated a subsection of all parameters that influence the overall drying potential of an EIFS clad wall. The major assumptions employed in this study were a particular airflow path (the interior and exterior cracks) and the constant interior temperature and relative humidity of 21°C and 45%, respectively.

The drying performance of the wall system was simulated for two climatic conditions, representing cold and mixed climates, and two stud cavity insulation systems, one hygroscopic and the other nonhygroscopic. Results drawn from this study assessed the effect of climatic location and stud cavity insulation on the hygrothermal performance of a particular EIFS clad wall. Results showed that air leakage through an EIFS clad wall in Wilmington produced a net drying effect for an initially wet OSB layer while developing a net seasonal accumulation in Chicago. However, while air leakage may be beneficial for the drying out of this particular wall system in Wilmington, there is an associated energy cost (sensible and latent heat loads). The two simulation cases effectively demonstrated the effect of climate on the positive/neutral and negative consequences of air leakage.

The effect of stud cavity insulation was also found to be critical, as the storage capacity for moisture increased in the cellulose case compared to the fiberglass insulation case. The amount of air leakage was also reduced in the cellulose insulation case due to the lower insulation air permeability. The net effect when comparing the two insulation systems was that the cellulose insulation case retained higher amounts of moisture that could lead to more rapid moisture-induced problems. Solar-driven moisture was more likely to be stored within the insulation and wood plates than being diffused outward to the exterior. However, if the OSB layer was installed dry and not wet, the observations of moisture storage within the cellulose could be significantly reduced.

A state-of-the-art model, linking thermal and moisture effects with the risk of moisture-induced damage, was presented in the form of a mold growth index. The results show the probable mold growth index potential as a function of climatic conditions and as a function of cavity insulation. A higher risk of mold growth may be present in the cellulose case than the fiberglass insulation case. For the same wall system, Wilmington exhibited slightly worse conditions than Chicago for mold growth.

Further research is recommended to determine the effect of various air leakage paths, the effect of water penetration through cracks, the effect of a wider range of climatic condi-

tions, the effect of exterior insulation thickness, and the influence of the presence of a vented cavity on the drying performance of an EIFS wall. The results provided in this paper are only applicable to the specific materials, initial conditions, airflow paths, wall orientation, wall specifications, and weather conditions employed in this study.

REFERENCES

ASC. 1993. *Theory documentation for TASCflow, Version 2.2*. Waterloo, Canada: Advanced Scientific Computing, Ltd.

Hamlin, T., and J. Gusdorf. 1997. Airtightness and energy efficiency of new conventional and R-2000 housing in Canada. Report, CANMET Energy Technology Center, Ottawa.

Hens, H., and A. Janssens. 1993. Inquiry on HAMCAT CODES. Heat, air and moisture transfer in insulated envelope parts. Report, Annex 24, Task 1, Modelling, International Energy Agency.

Hukka, A., and H. Viitanen. 1998. A mathematical model of mold growth on wooden material. Submitted to *Wood Science.*

Janssens, A., and H. Hens. 1996. Condensation and airtightness: Tolerance of roof design. *Building Physics in the Nordic Countries, Espoo, Finland, September 9-10*, pp. 423-430.

Karagiozis, A. 1997. Porous media transport. *CFD 97, The Fifth Annual Conference of the Computational Fluid Dynamics Society of Canada, Victoria, May 25-27*, pp. 7-21 to 7-25.

Karagiozis, A. 1993. Overview of the 2-D hygrothermal heat-moisture transport model LATENITE. Internal IRC/BPL Report.

Karagiozis, A.N., and H.M. Salonvaara. 1998. Hygrothermal performance of EIFS walls: Effect of the combined vapor diffusion and air leakage on the drying potential of an EIFS wall. Third Symposium on Water Problems in Building Exterior Walls: Evaluation, Prevention and Repair. STP1352, American Society for Testing and Materials.

Karagiozis, A.N., and M.K. Kumaran. 1997. Drying potential of EIFS walls: Innovative vapor control strategies. Exterior Insulation and Finish Systems (EIFS): Innovations and Solutions to Industry Challenges. STP1339, American Society for Testing and Materials.

Karagiozis, A., M. Salonvaara, and K. Kumaran. 1994. LATENITE hygrothermal material property database. IEA Annex 24 Report T1-CA-94/04, Trondheim, Norway.

Kim, A.K., and C.Y. Shaw. 1986. Seasonal variation in ai tightness of two detached houses. Measured Air Leal age of Buildings, ASTM STP 904, 17. H.R. Trechs and P.L. Lagus, eds. Philadelphia: American Society f Testing and Materials.

NCC. 1995. Data for Wilmington, N.C. National Climat Center.

Nisson, N.J.D. 1995. Severe rotting found in homes wi exterior insulation systems. *Energy Design Update*, Vc 15, No. 12 (Dec.), pp.1-3.

Ojanen, T., and M.K. Kumaran. 1996. Effect of exfiltratic on the hygrothermal behavior of a residential wa assembly. *J. Thermal Insul. and Bldg. Envs.* 9: 215-22

Ojanen, T., and M.K. Kumaran. 1992. Air exfiltration an moisture accumulation in residential wall cavities. *The mal Performance of the Exterior Envelopes of Building V.* Atlanta: American Society of Heating, Refrigeratin and Air-Conditioning Engineers, Inc.

Persily, A.K. 1986. Measurements of air infiltration and ai tightness in passive solar homes. Measured Air Leakag of Buildings. ASTM STP 904, 46. H.R. Trechsel an P.L. Lagus, eds. Philadelphia: American Society c Testing and Materials.

Salonvaara, M., and A. Karagiozis. 1994. Moisture transpo in building envelopes using an approximate factoriz tion solution method. CFD Society of Canada, Toronto June 1-3.

Straube, J.F. 1998. Moisture control and enclosure wall sys tems. Ph.D. thesis, University of Waterloo, Waterloo Ontario, Canada.

TenWolde, A., and W.B. Rose. 1996. Moisture control strat egies for building envelope. *J. Thermal Insul. and Bldg Envelopes*, 9: 206-214.

Viitanen, H. 1997a. Modeling the time factor in the develop ment of brown rot decay in pine and spruce sapwood– The effect of critical humidity and temperature condi tions. *International Journal of the Biology, Chemistr and Technology of Wood* 51(2): 99-106.

Viitanen, H. 1997b. Modeling the time factor in the develop ment of mould fungi—The effect of critical humidity and temperature conditions on pine and spruce sap wood. *International Journal of the Biology, Chemistr and Technology of Wood* 51(1): 6-14.

Viitanen, H. 1996. Factors affecting the development o mould and brown rot decay in wooden material and wooden structures: Effect of humidity, temperature and exposure time, Ph.D. thesis.

Warren, P.R., and B.C. Webb. 1986. Ventilation measure ments in housing. CIBSE Symposium, Natural Ventila tion by Design. Chartered Institution of Building Services Engineers, London.